Crossing the ridge: How does the Widom line affect the physical behavior of supercritical fluids?

MATTHIAS IHME

Department of Mechanical Engineering, Stanford University
Department of Photon Science, SLAC National Accelerator Laboratory

Supercritical Fluids

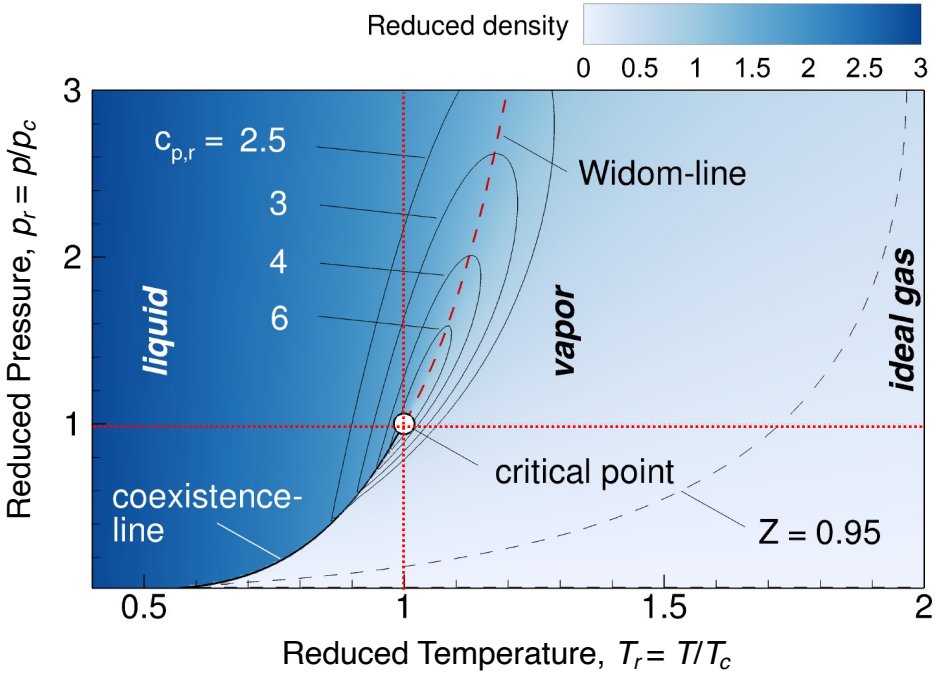

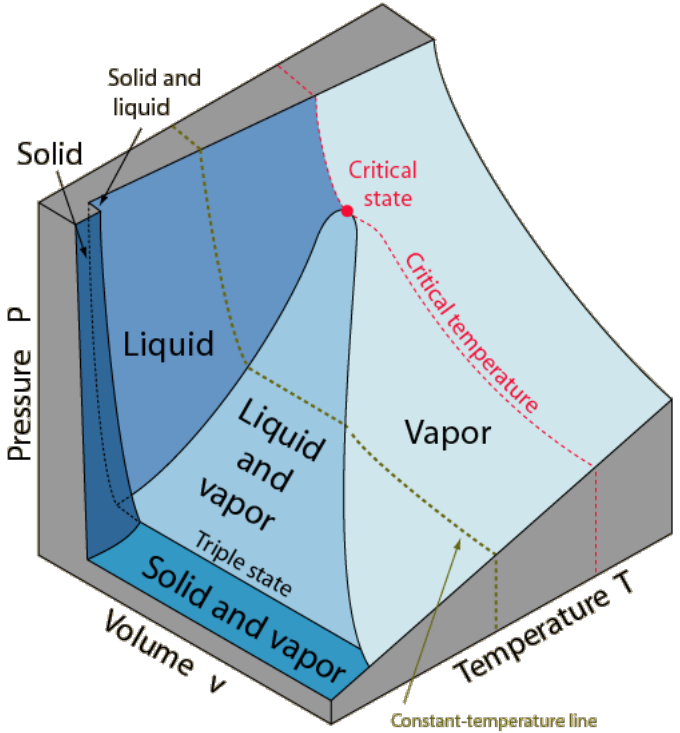

Supercritical Fluids

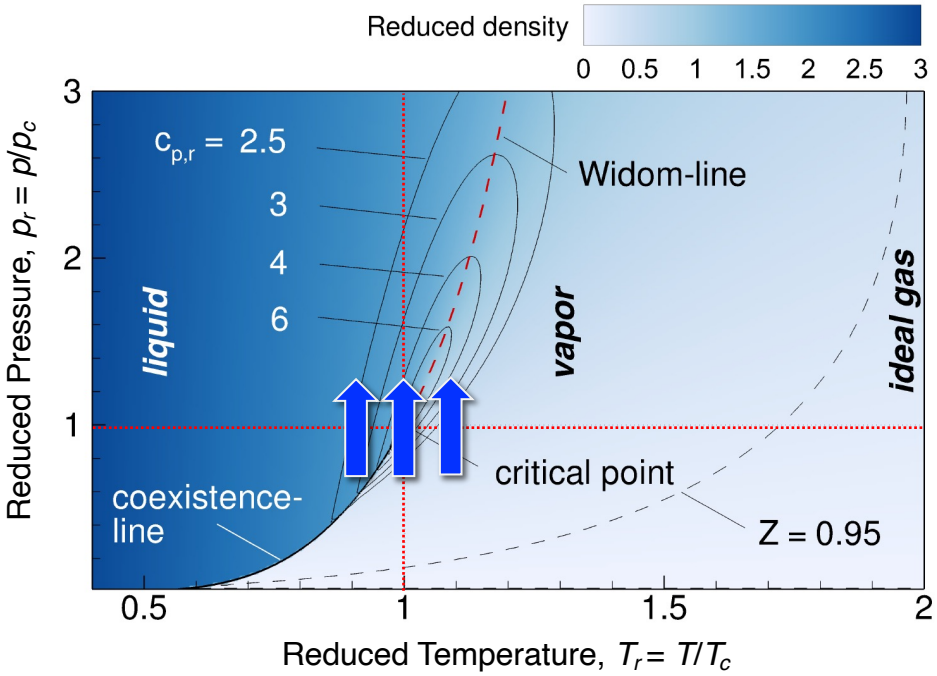

Transcritical pressure

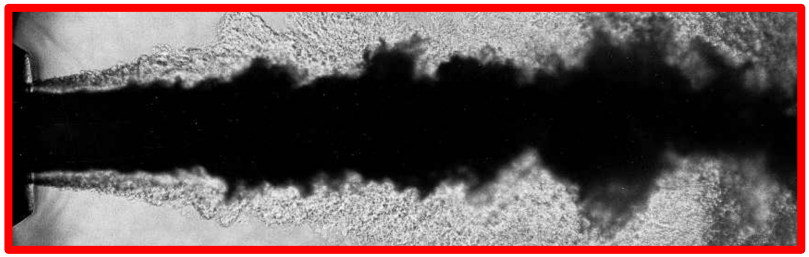

Subcritical pressure

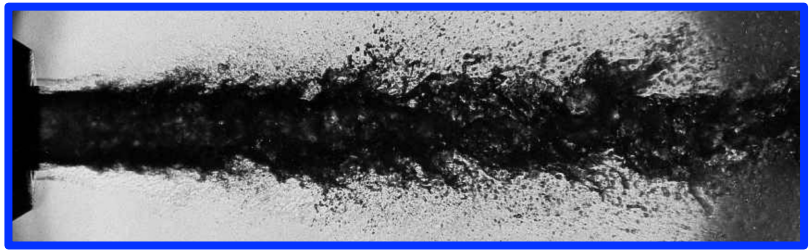

Supercritical Fluids

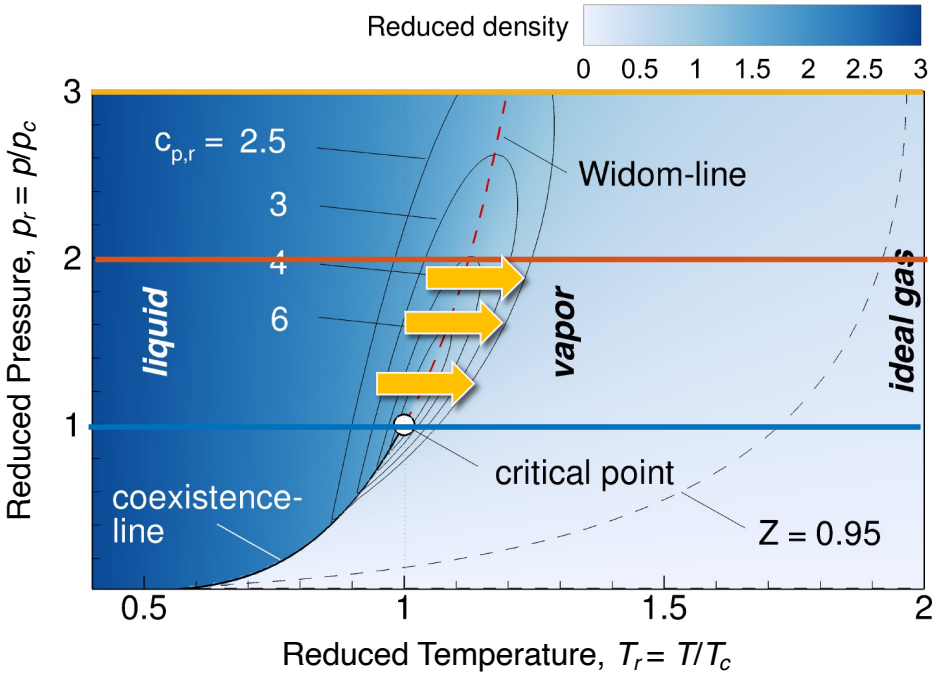

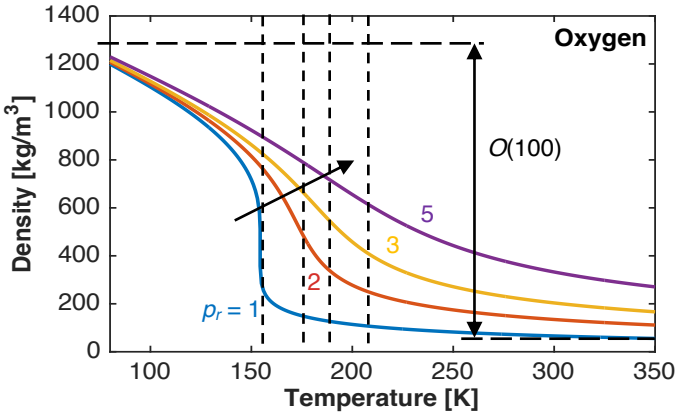

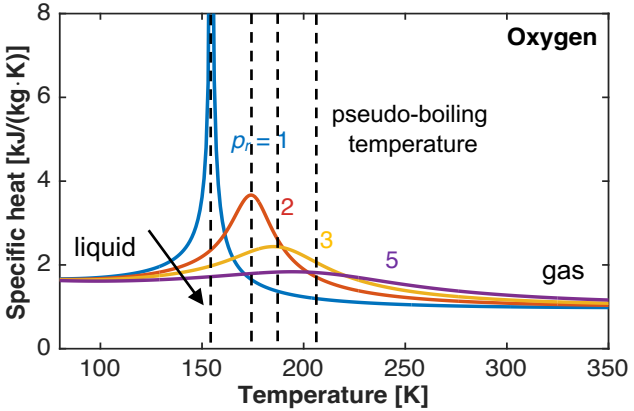

Role of Widom line on physics of supercritical fluids

- Strong variations in thermodynamic response functions affect different processes in high-pressure systems

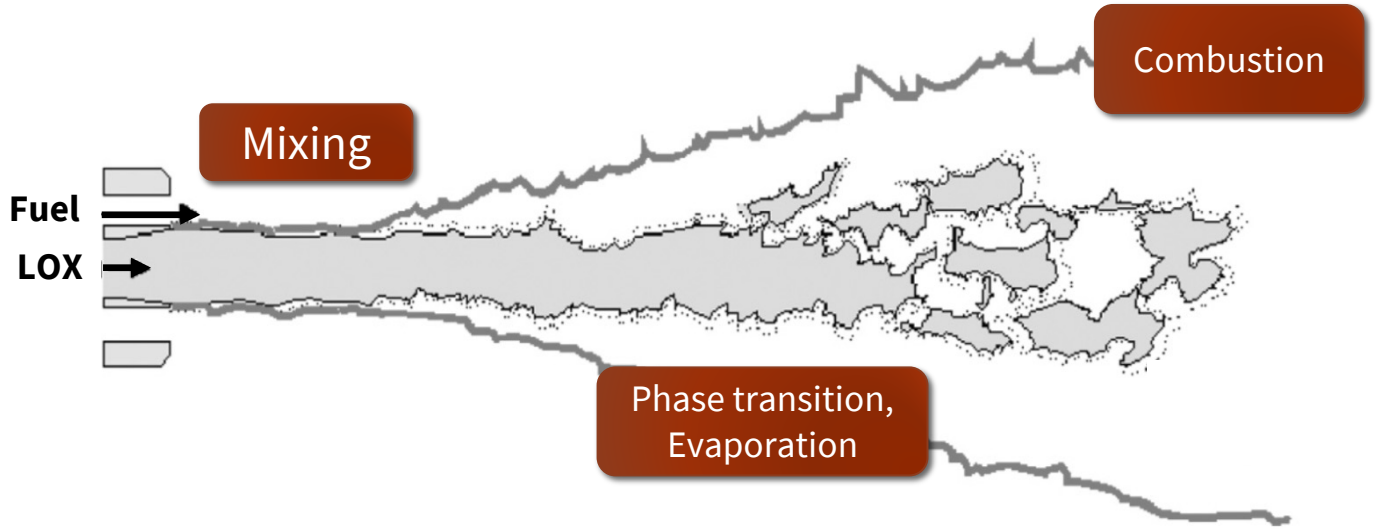

Mixing

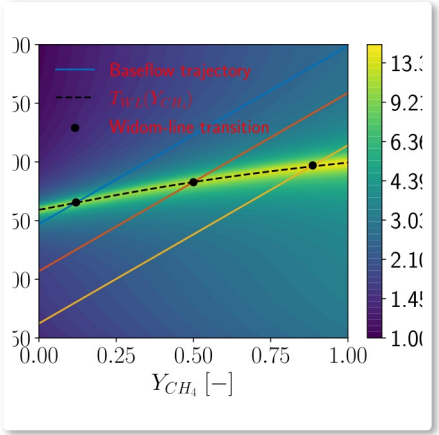
Baseflow trajectory
$T_{W,1}(Y_{CH_4})$
Widom-line transition
0.00
0.25
0.50
0.75
1.00
Y_{CH_4} [−]

Mixing at Supercritical Conditions

- Role of supercritical dense-fluid mixing in propulsion systems ➔ enhance sensibility of fluid response by real-fluid effects near Widom line

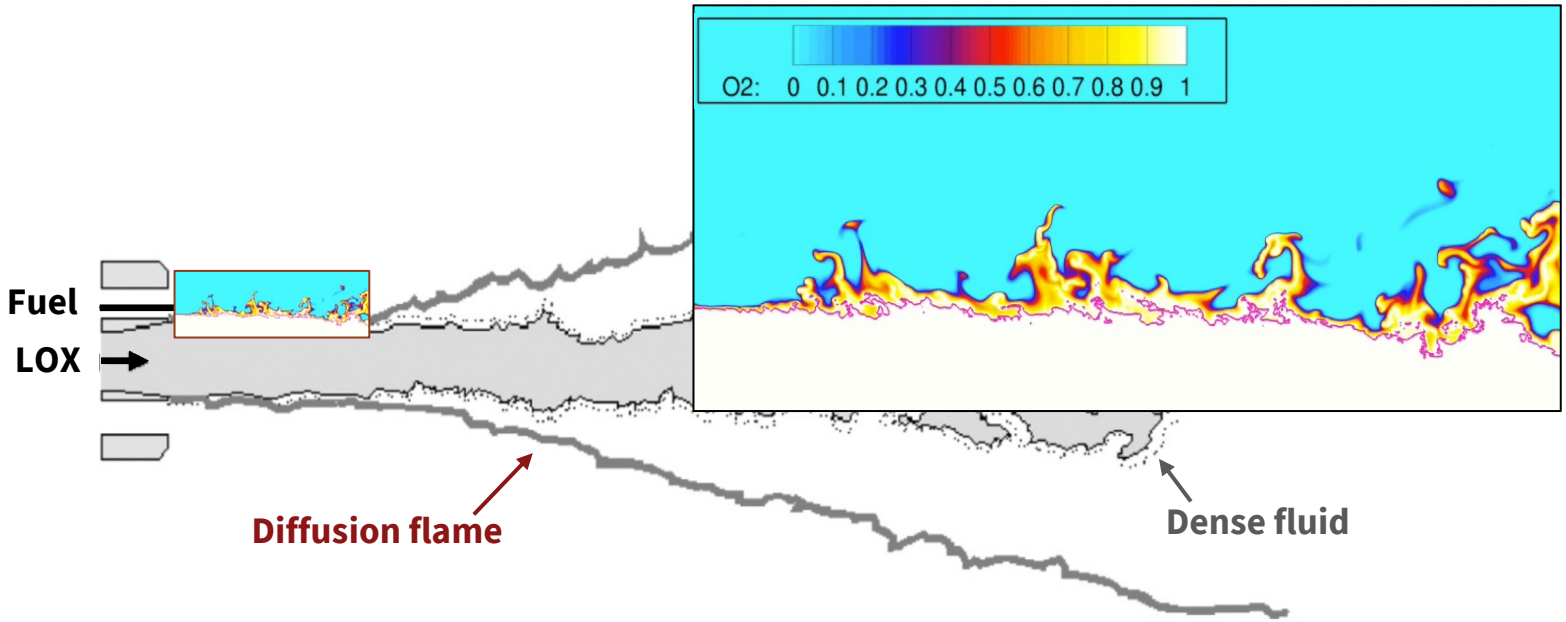

Supercritical Mixing Layer Stability

Research issue:

- Supercritical phase behavior is more complicated in binary systems
- Critical point and Widom line become functions of composition → mixing layer profile can cross Widom line at different locations

Research question: How does the attunement of Widom line transition at different locations of the laminar mixing layer influence its stability?

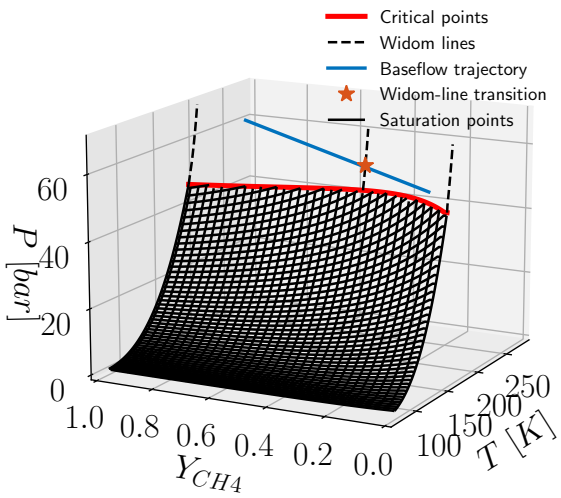

Ly and Ihme "Destabilization of binary mixing layer in supercritical conditions." JFM, 945, 2022.

Supercritical Mixing Layer Stability

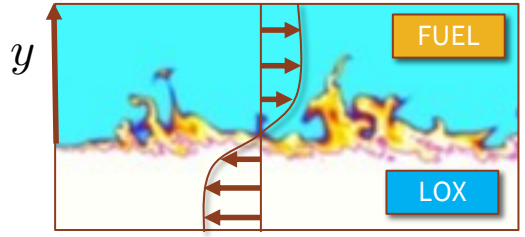

Physical insight from linear stability analysis

- Consider LOX/CH4 shear-layer
- Linearize governing equations about locally parallel base-flow

$$\phi(\boldsymbol{x},t) = \overline{\boldsymbol{\phi}}(y) + \boldsymbol{\phi}'(\boldsymbol{x},t)$$

- Normal-mode expansion and spatial stability analysis

$$\boldsymbol{\phi}'(\boldsymbol{x},t) = \widehat{\boldsymbol{\phi}}(y)\exp\{-i(\omega t - \alpha x)\}$$

Complex-valued wave number

$$\alpha_i = \begin{cases} < 0: & \text{unstable} \\ > 0: & \text{stable} \end{cases}$$

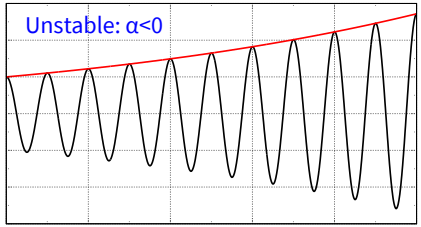

Supercritical Mixing Layer Stability

Physical insight from linear stability analysis

- Vary baseflow centerline temperature to control location of Widom line transition y_{WL} $\quad \overline{T}(y) = T_{\mathrm{ctr}} + \Delta_T \tanh(y)$

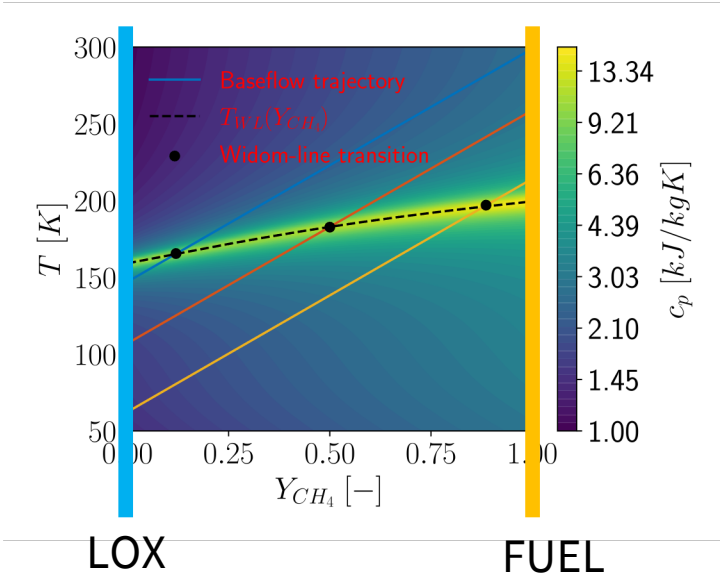

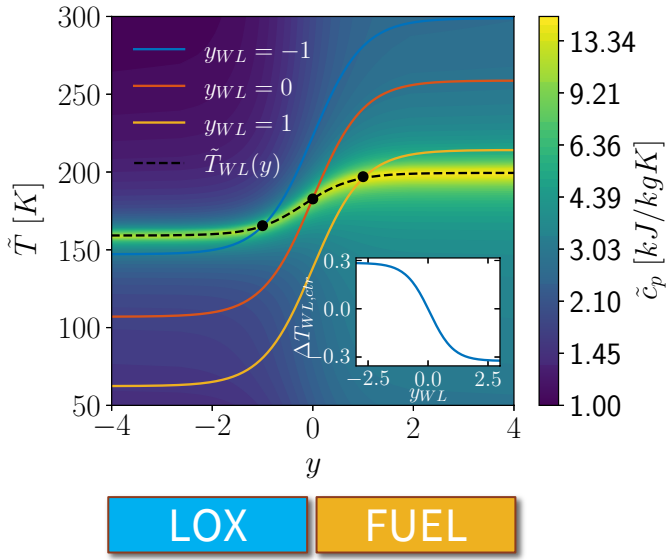

Supercritical Mixing Layer Stability

Effects of pressure variation

- Dual-mode instability mechanism
- At near critical pressure: Widom-line-induced structure destabilize flow

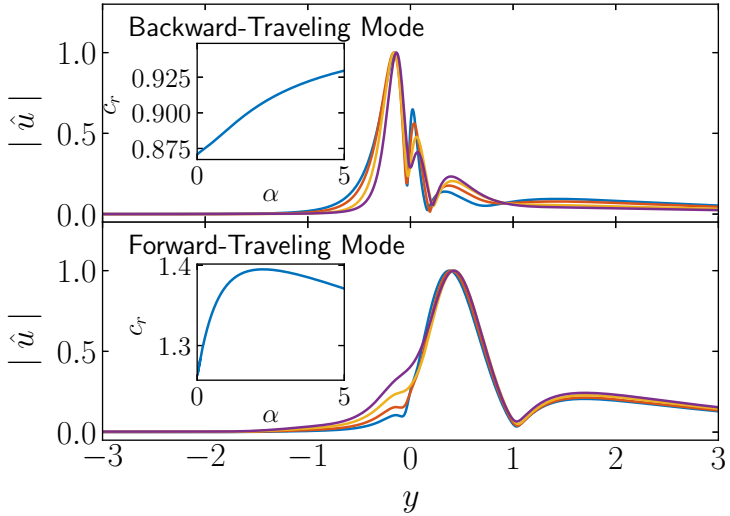

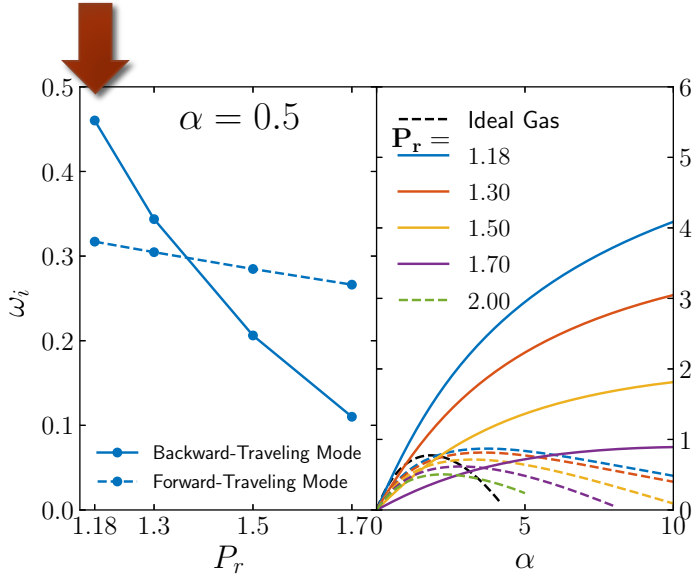

Supercritical Mixing Layer Stability

Widom-line attunement

- Destabilization of shear layer by Widom-line attunement due to secondary thermodynamically induced instability mode

$y_{WL} = 0$ $y_{WL} = -0.5$ $y_{WL} = -3$

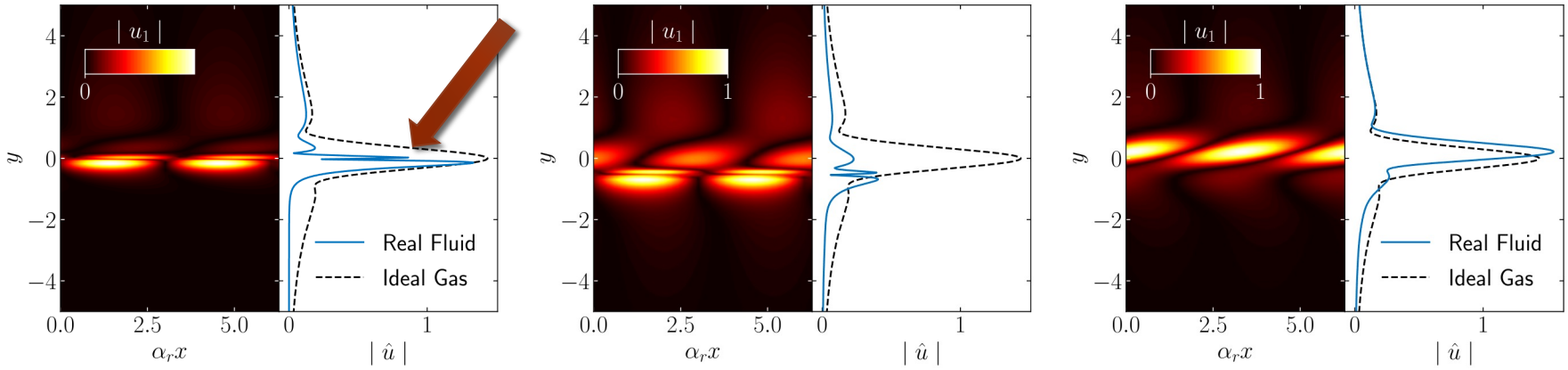

Supercritical Mixing Layer Stability

- Second-order phase transition across Widom line results in enhanced thermodynamic response
  - Flow destabilization by thermodynamic-induced instability mode
  - Mode decays with increasing pressure above and with detuning of Widom-line transition location away from hydrodynamic inflection point

➔ Opportunities for modulating shear-layer instabilities in supercritical flow!

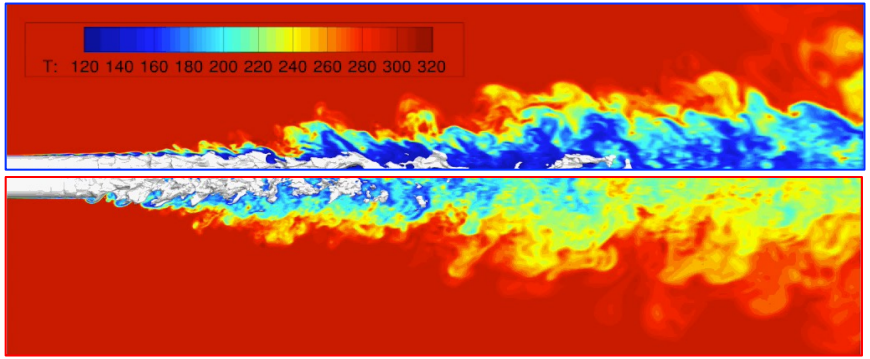

Ly and Ihme "Destabilization of binary mixing layer in supercritical conditions." JFM, 945, 2022.

Phase transition

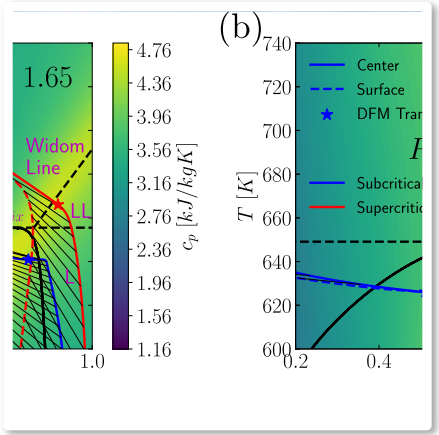

Droplet Evaporation

Injection of liquid fuel into ambient environment at supercritical pressure conditions

- **Subcritical evaporation:** strong influence of sharp liquid-vapor interface, latent heat of vaporization, and surface tension
- **Dense-fluid mixing:** Interfacial dynamics no longer present → mixing of a dense gas-like fluid

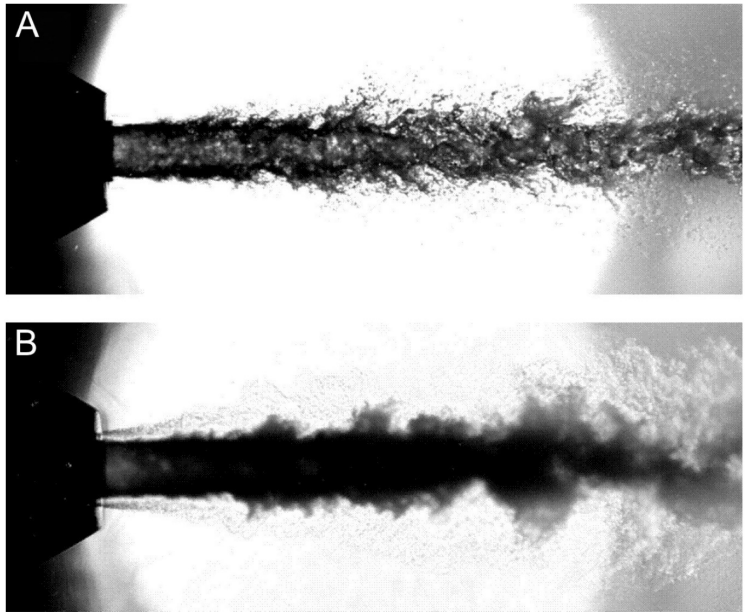

Mayer & Smith, 2004

Droplet Evaporation

- Robust criterion needed to distinguish subcritical evaporation and supercritical dense fluid mixing
  - Experimental: Disappearance of material surface
  - Theoretical: Mixing trajectory exceeds two-phase region

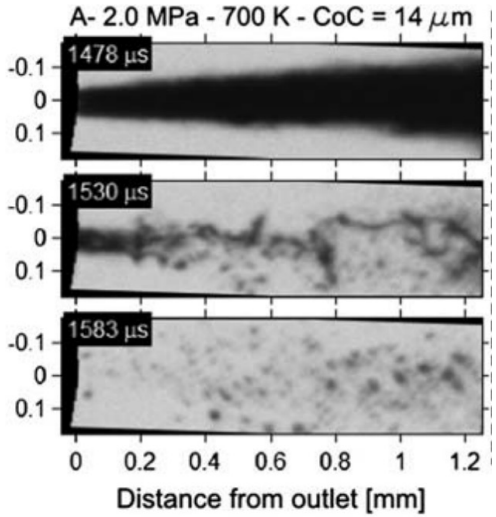

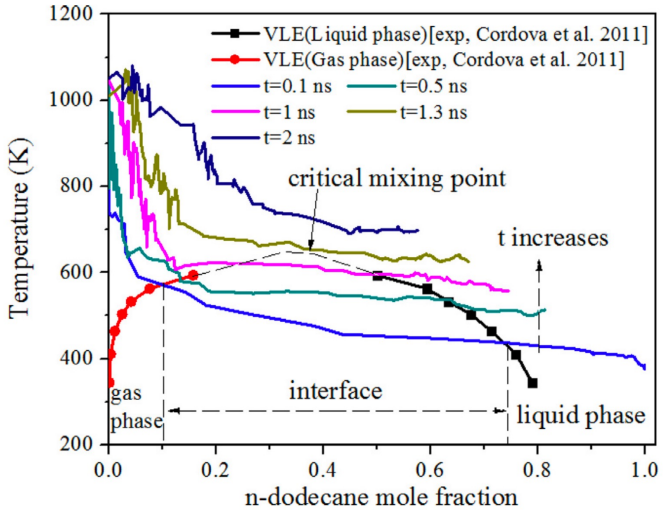

Mo & Qiao, 2017
Manin et al., 2014

Droplet Evaporation

Objective

- Conduct detailed numerical analysis of thermotransport dynamics during transition from subcritical evaporation to supercritical dense fluid mixing
- Uncover dense-fluid mixing behavior

Approach

- Consider microgravity nanodroplet configuration: $R_0 = 20 - 120nm$
- Use interface resolving continuum-based formulation to describe transcritical dynamics
- Model non-local thermodynamics induced by molecular interactions across the high-gradient interface

Governing Equations

- Interface resolving diffuse interface method contains both traditional stress and species and energy diffusion fluxes $(\boldsymbol{\tau}, \boldsymbol{J}_1, \boldsymbol{q})$ and interfacial stress and fluxes $(\boldsymbol{K}, \boldsymbol{\mathfrak{J}}_1, \boldsymbol{\mathfrak{Q}})$

$$\frac{D\rho}{Dt} = -\rho(\nabla \cdot \boldsymbol{v}),$$
$$\rho \frac{D\boldsymbol{v}}{Dt} = -\nabla P_{GD} + \nabla \cdot (\boldsymbol{\tau} + \boldsymbol{K}),$$
$$\rho \frac{DY_1}{Dt} = -\nabla \cdot (\boldsymbol{J}_1 + \boldsymbol{\mathfrak{J}}_1),$$
$$\rho \frac{DE}{Dt} = -\nabla \cdot (P_{GD}\boldsymbol{v}) - \nabla \cdot (\boldsymbol{q} + \boldsymbol{\mathfrak{Q}}) + \nabla \cdot [(\boldsymbol{\tau} + \boldsymbol{K}) \cdot \boldsymbol{v}]$$

- Interfacial terms scale with the capillary coefficient → automatically vanishes in regions away from liquid-interface or where interface does not exist (supercritical condition)

Ly, Majumdar, Ihme "Regimes of evaporation and mixing behaviors of nanodroplets at transcritical conditions." Fuel, 2023

Verification

- Numerical simulation of interfacial structure and dynamics are compared against MD results for both equilibrium interface and evaporating nanodroplets
- Further validation of phase-exchange simulation via comparison with a transcritical millimeter-scale droplet evaporation experiment. Here, the simulated droplet radius is $R_0 = 120\,nm$. This demonstrates the convergence to d_0^2-scaling.

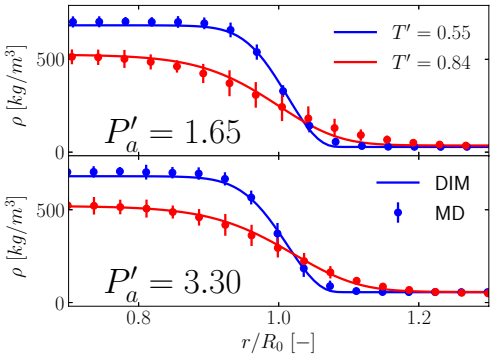

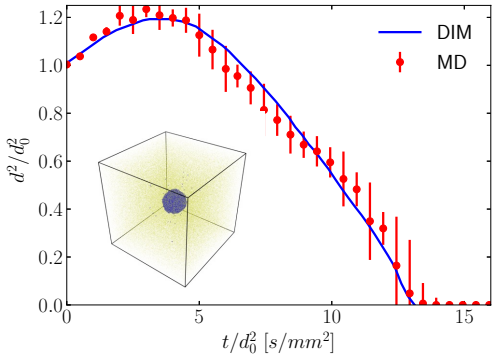

$R_0 = 10nm, R_a/R_0 = 3$

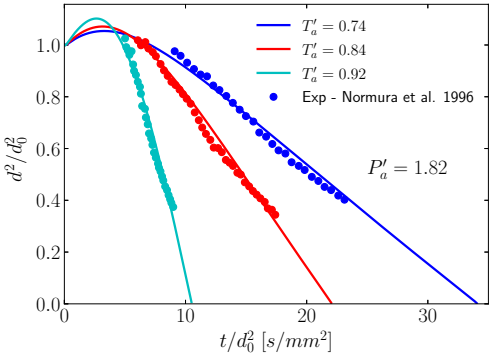

$R_0 = 120nm, R_a/R_0 = 20$

Transcritical phase-exchange behavior

Phase-exchange mechanisms:

- Subcritical evaporation (▽): Retraction of a subcritical surface
- Supercritical evaporation (△): Retraction of supercritical surface
- Subcritical DFM (○): Diffusion of a uniform gaseous fluid
- Supercritical DFM (◇): Diffusion of a uniform gas-like fluid

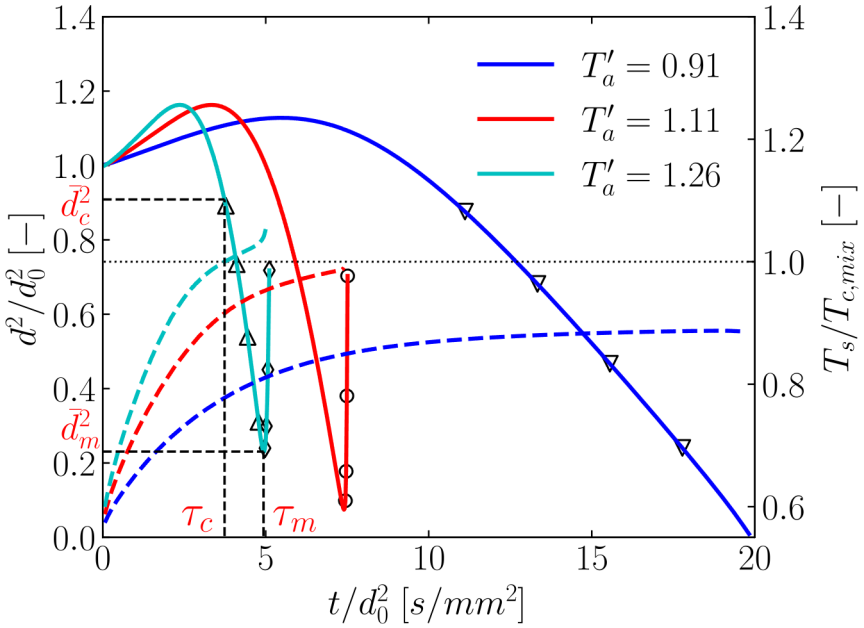

Transcritical phase-exchange behavior

- Subcritical Evaporation: Sharp interface with distinct material and compositional surface
- Supercritical Evaporation: Supercritical surface. Compositional surface vanishes
- Subcritical/Supercritical DFM: Diffusion of uniformly gaseous/gas-like fluid. Thus, there is no apparent material or compositional surface.

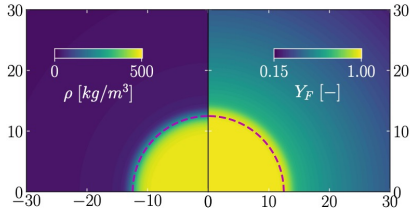

(a) Subcritical Droplet. t = 12 ns.

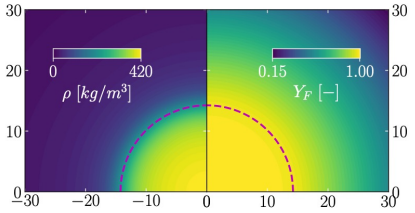

(b) Supercritical Droplet. t = 3.4 ns.

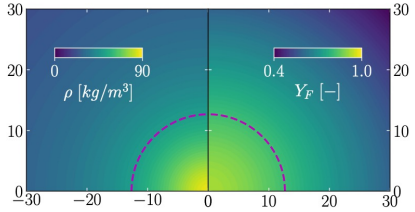

(c) Subcritical DFM. t = 6.76 ns.

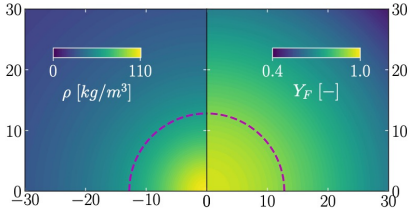

(d) Supercritical DFM. t = 4.60 ns.

Regime map of dominant behaviors

- I: Monolithic subcritical evaporation
- II: Transition to subcritical DFM at the end of the subcritical evaporation period
- III: Transcritical evaporation
  - III-a: Dominated by supercritical evaporation
  - III-b: Dominated by supercritical DFM.
- Boundaries for regimes I and III-a, III-b are insensitive to droplet sizing.

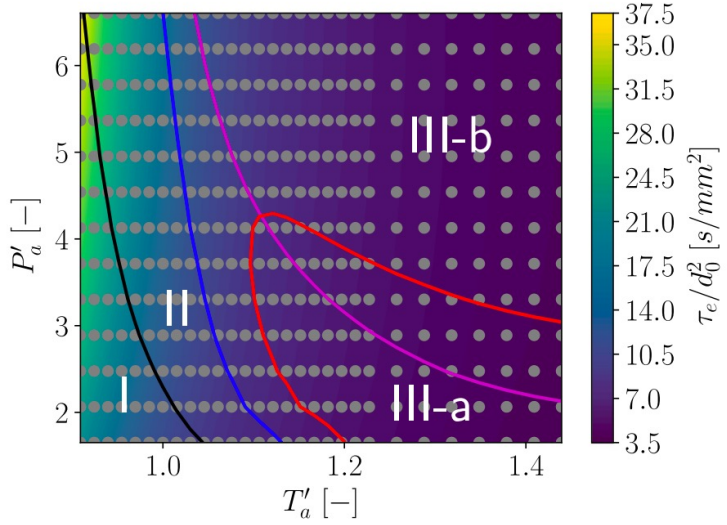

Ly, Majumdar, Ihme "Regimes of evaporation and mixing behaviors of nanodroplets at transcritical conditions." Fuel, 2023

Combustion

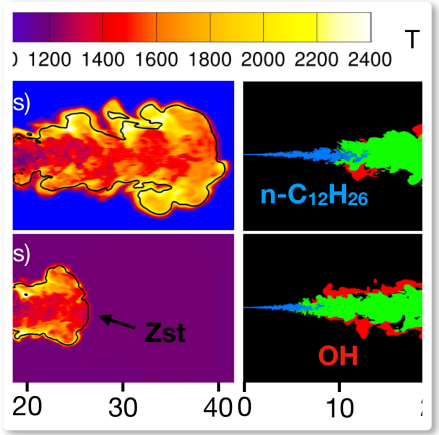
T
1200 1400 1600 1800 2000 2200 2400
n-C12H26
Zst
OH
20
30
40
0
10

Transcritical Injection in Diesel Engines

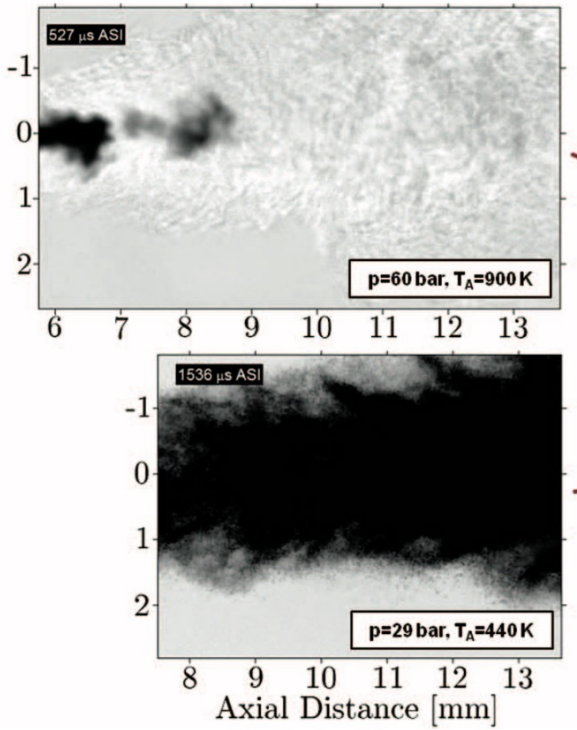

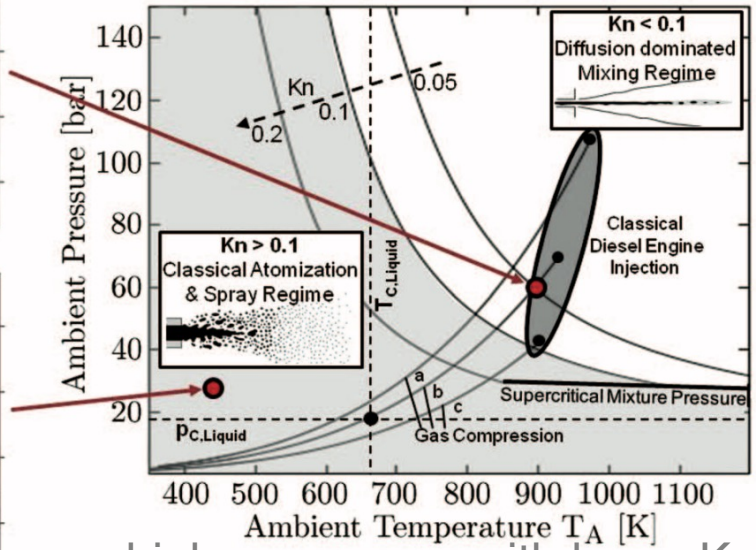

higher pressure with lower Kn number

➠ interfacial diffusion layer

Pickett, L. M. & Bruneaux, G. Engine Combustion Network, *www.sandia.gov/ECN* (2011)
Dahms, R. N. & Oefelein, J. C. *Phys. Fluids* **25**, 092103 (2013)
Manin J., Bardi, M., Pickett, L. M., Dahms, R. N., Oefelein, J. C. *Fuel* **134**, 531-543 (2014)

Transcritical Injection in Diesel Engines

- Examine effects of high-pressure environment on combustion
  - kinetics-controlled transient auto-ignition process
- Combine diffuse-interface method with finite-rate chemistry model
- 54-species n-dodecane/air skeletal mechanism
  - Further reduced by setting 21 species in QSS approximation

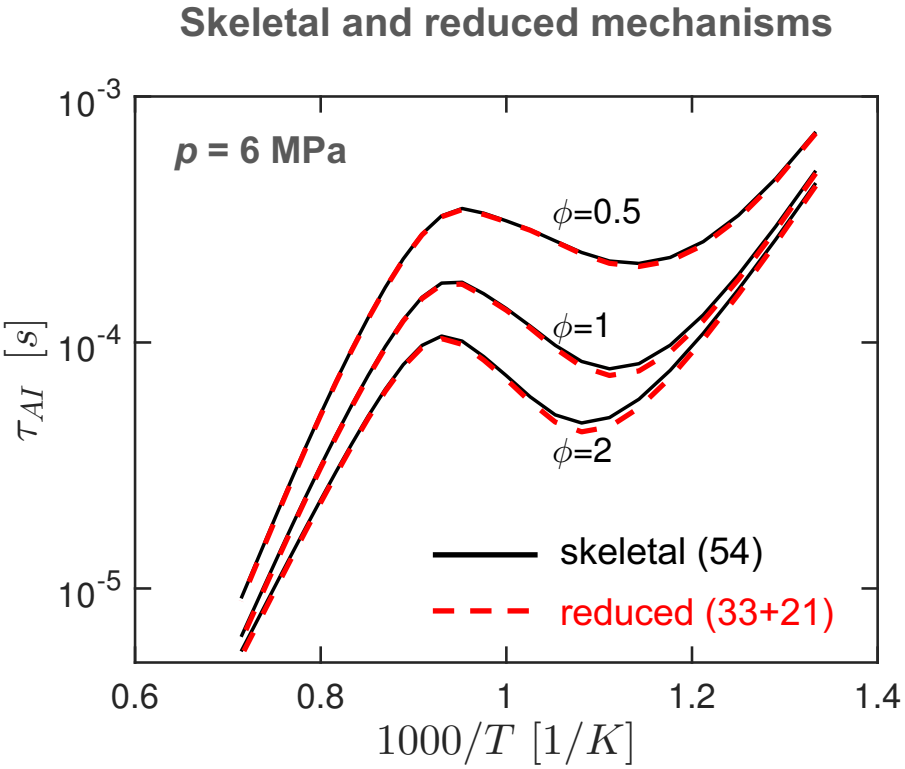

Yao, T., Pei, Y., Zhong, B.-J. et al. *Fuel* **191**, 330-349 (2017)

Experimental & Numerical Setup

- Bosch injector with a nominal diameter of 0.09 mm for the nozzle
- Cylinder domain (40 mm x 80 mm) with 8.7 million cells and minimum spacing of 4 μm

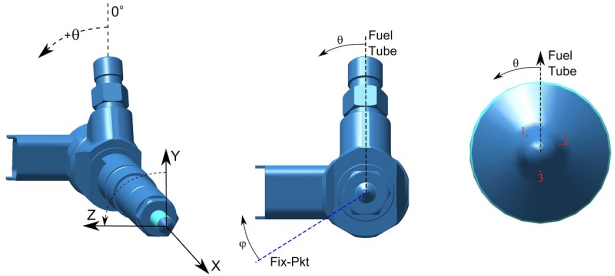

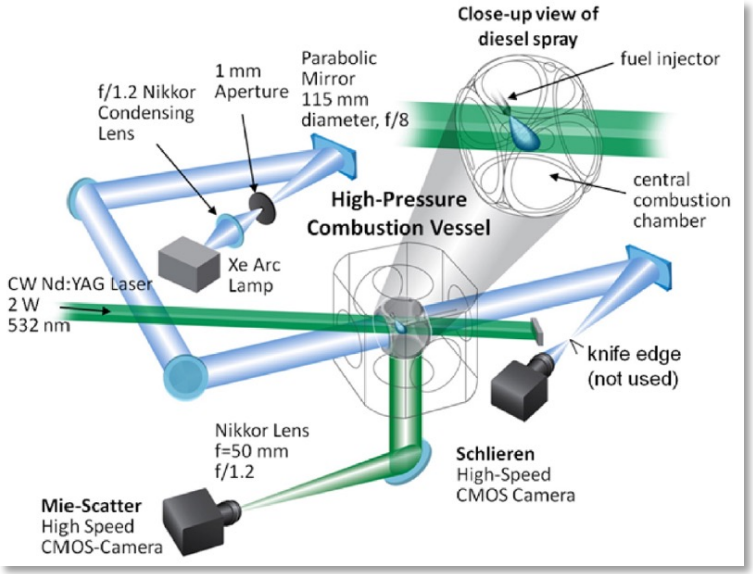

Sandia Spray Combustion Chamber

Pickett, L. M. & Bruneaux, G. Engine Combustion Network, *www.sandia.gov/ECN* (2011)

Experimental & Numerical Setup

- Bosch injector with a nominal diameter of 0.09 mm for the nozzle
- Cylinder domain (40 mm x 80 mm) with 8.7 million cells and minimum spacing of 4 μm
- 363 K *n*-dodecane fuel injected into 900-1200 K ambient with 0% (inert) and 15% (reacting) O_2 at 6 MPa
- Time-dependent inflow mass flux following ECN recommendations
- 4th-order semi-implicit Rosenbrock-Krylov scheme for integrating reaction chemistry
- LES SGS closure
  - Vreman SGS model
  - Dynamic thickened-flame model with maximum thickening factor set to be 4

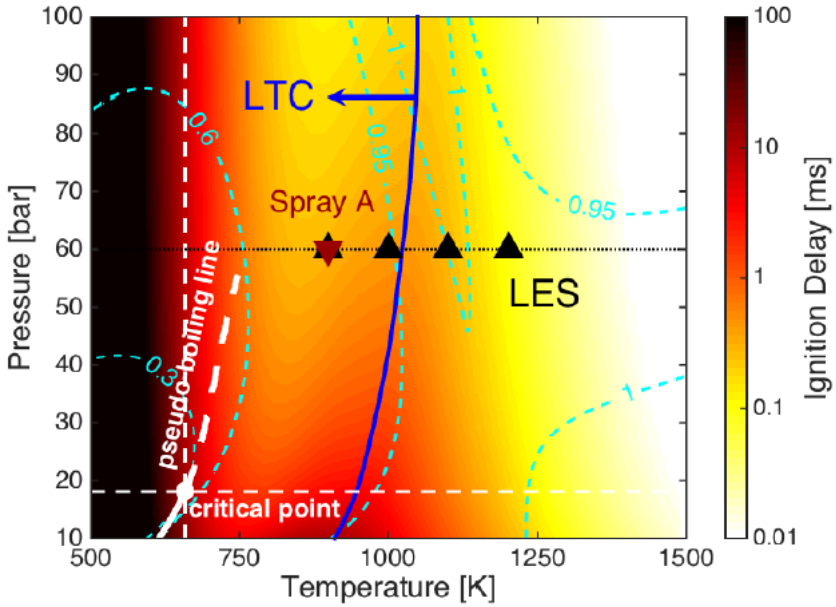

Operating conditions

Pickett, L. M. & Bruneaux, G. Engine Combustion Network, *www.sandia.gov/ECN* (2011)
Colin, O., Ducros, F., Veynante, D., Poinsot, T. Phys. Fluids **12**(7), 1843–1863 (2000)

Injection Sequence for Inert Spray A Case

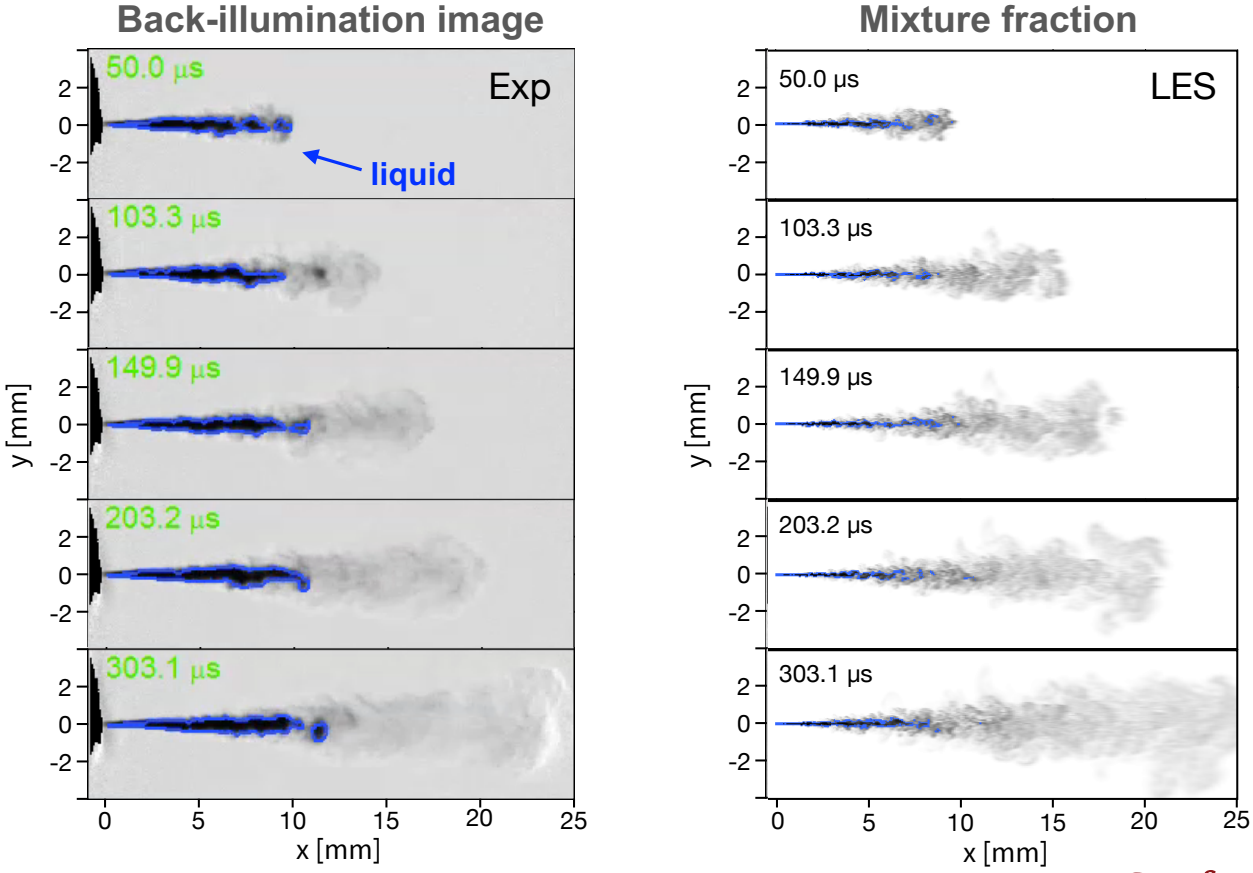

Manin, J., Bardi, M., Pickett, L. M. *COMODIA2012* (2012)

Penetration Lengths

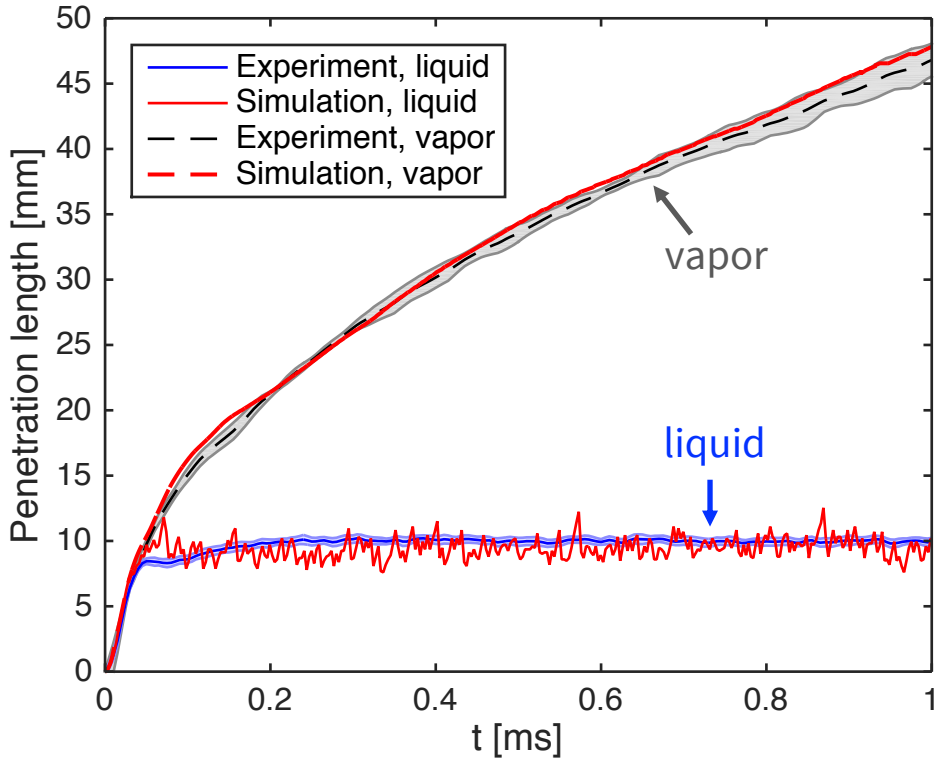

Pickett, L. M., Kook, S., Williams, T. C. *SAE Int. J. Engines* **2**(1), 439-459 (2009)

Auto-ignition Sequence for Reacting Case

- Auto-ignition case with 900 K ambient temperature and 15% O_2
- Low-temperature chemistry (cool flame) region represented by formation of CH_2O species
- OH species formed at the edges of the penetrating jet

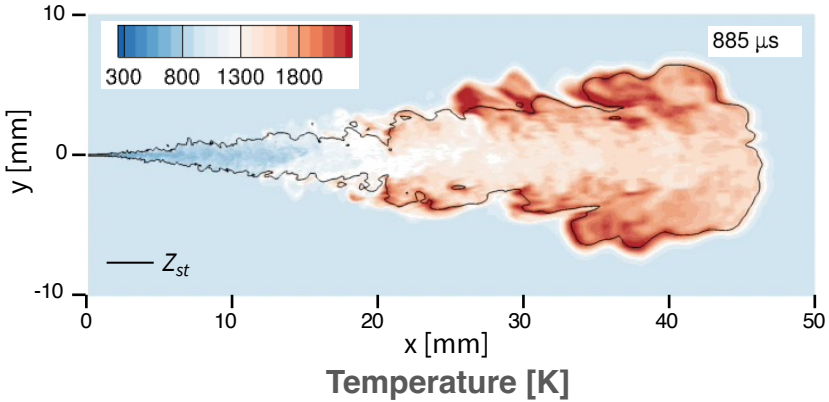

Auto-ignition Sequence for Reacting Case

- Auto-ignition case with 900 K ambient temperature and 15% O_2
- Low-temperature chemistry (cool flame) region represented by formation of CH_2O species
- OH species formed at the edges of the penetrating jet

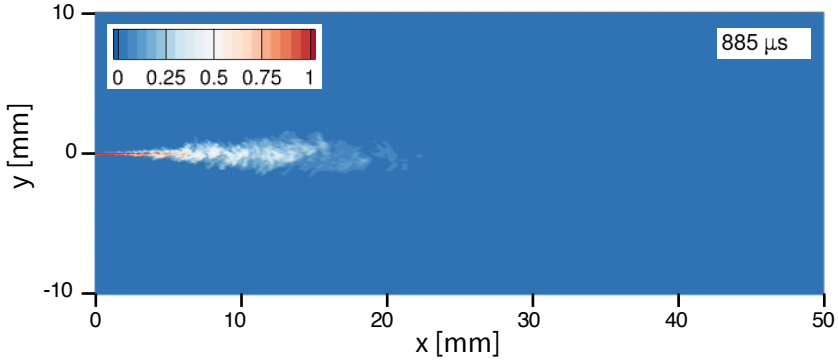

n-Dodecane mass fraction

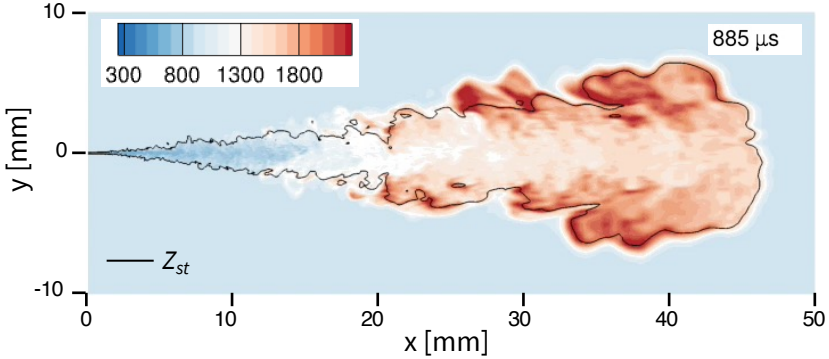

Temperature [K]

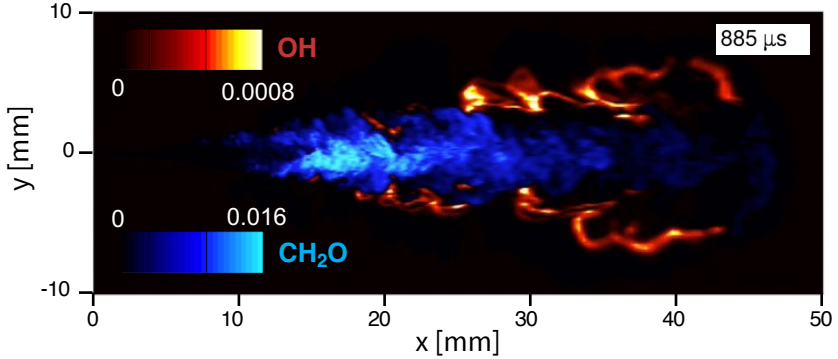

CH_2O and OH mass fractions

Ma, Wu, Jaravel, Bravo, Ihme, Proc. Combust. Inst., 37, 2019, 3303-3310.

Temperature Field and Species Distribution

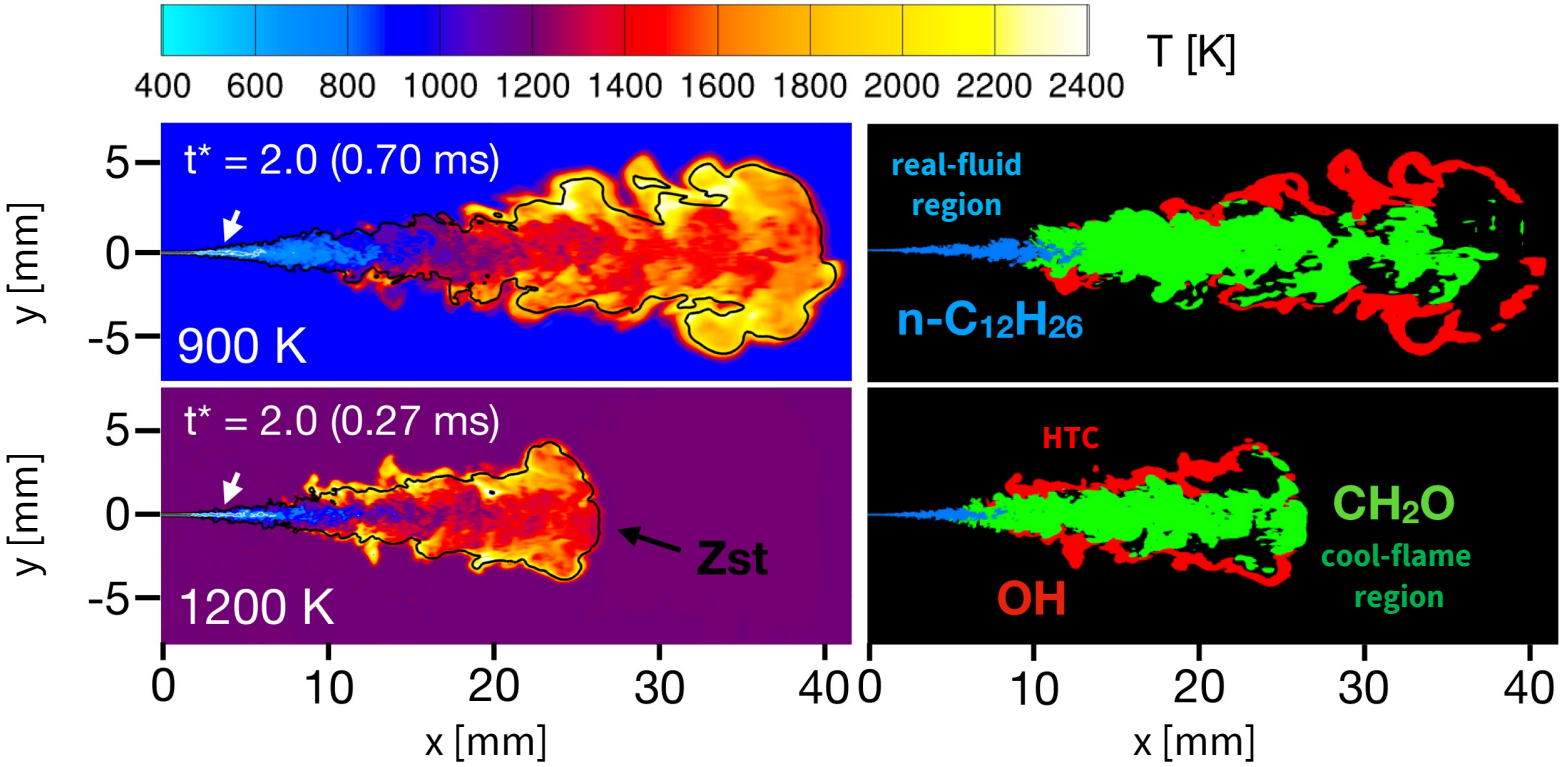

t* is the time normalized by corresponding ignition delay

White contours represent real-fluid regions (5% deviation from unity compressibility factor)

Ignition Delay Time Prediction

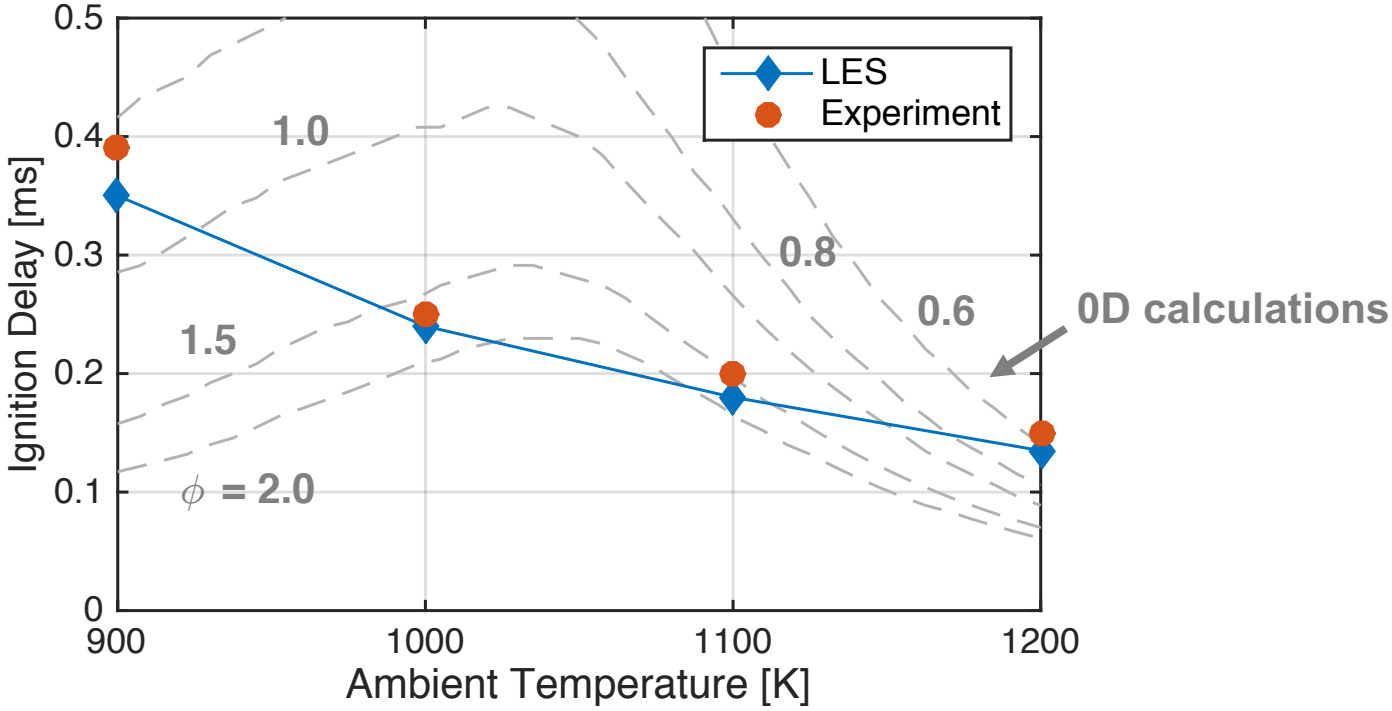

› Ignition delay in LES is defined as the time when the maximum OH mass fraction reaches 14% of the value at quasi-steady state of the flame following ECN-recommendations

Chung, Ma, Ihme, "Examination of diesel spray combustion in supercritical ambient fluid using large-eddy simulations." Int. J. Eng. Res. 21, 2020.

Summary and Conclusions

- A diffuse-interface method in conjunction with a finite-rate chemistry model for modeling diesel fuel injection and auto-ignition processes at transcritical conditions
  - flow fields of the injection sequence and predicted vapor penetration length are qualitatively in good agreement with experimental results
  - Good agreement of the ignition delay time is obtained from simulation results at different ambient temperature conditions
  - The formation of intermediate species is captured by the simulations

- Combustion occurs at subcritical mixture conditions, far removed from Widom line
- Transport and mixing strongly affected by Widom-line effects

Research Challenges

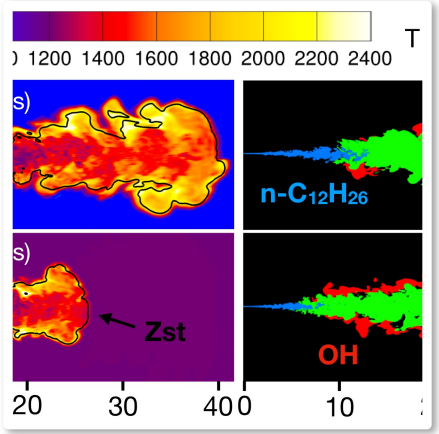

Opportunities and open research questions

Numerical algorithms and computational methods

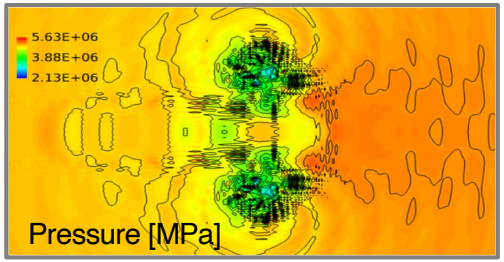

Thermofluid flows: heat transfer, turbulence, mixing properties

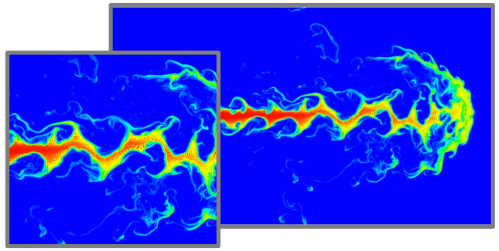

Experimental data: model evaluation, thermodynamic properties

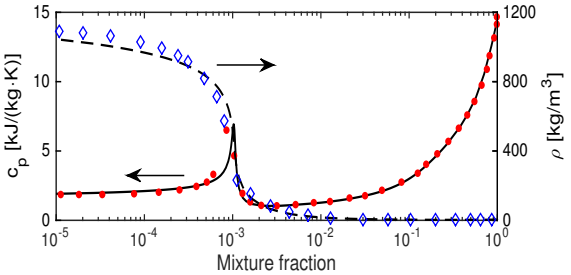

Ihme, Chung, Mishra, "Combustion machine learning: Principles, progress and prospects." Prog. Energy Combust. Sci. 91, 2022.

Role of Widom line on physics of supercritical fluids

- Mixing
- Phase Transition
- Heat transfer
- Combustion

Thank you!